# Clamping Force Effects on the Performance of Mechanically Attached Piezoelectric Transducers for Impedance-Based NDE

Charles M. Tenney[1, 2], Mohammad A. Albakri[1], Christopher B. Williams[2], and Pablo A. Tarazaga[1]

[1]Vibration, Adaptive Structures and Testing (VAST) Laboratory
Department of Mechanical Engineering
College of Engineering

[2] Design, Research, and Education for Additive Manufacturing Systems (DREAMS) Laboratory
Department of Mechanical Engineering
College of Engineering

Virginia Tech, Blacksburg, VA 24060

**ABSTRACT**
Impedance-based non-destructive evaluation (NDE) constitutes a generalization of structural health monitoring (SHM), where comparisons between known-healthy reference structures and potentially-defective structures are used to identify damage. The quantity considered by impedance-based NDE is the electrical impedance of a piezoelectric element bonded to the part under test, which is linked to the dynamic vibrational response of the part under test through electromechanical coupling. In this work, the piezoelectric element is not bonded directly to the part under test, but rather to a c-shaped clamp, which is then mechanically attached to the part under test. Under this attachment condition, the effect of clamping force on the sensitivity of the impedance-based evaluation is investigated for machined steel blocks with varying levels of damage severity. The highest clamping force tested (600 lb, 2670 N) was the only condition exhibiting increasing damage metric values with increasing damage severity in the parts under test, suggesting that higher clamping force increases sensitivity to damage.

**Keywords:** Electromechanical Impedance, Non-Destructive Evaluation, Piezoelectrics, Manufacturing Defects

## INTRODUCTION

Impedance-based non-destructive evaluation (NDE) is rooted in the field of structural health monitoring (SHM). Speaking generally, SHM involves first evaluating a given structure as-built to obtain a 'baseline' state. Periodically thereafter, evaluations of the structure can be gathered and compared to the baseline. Deviations from the baseline indicate changes in the structure, usually interpreted as damage. In increasing order of difficulty, this information may also be used to estimate the severity of damage, estimate the type and location of damage, estimate the remaining useful life of the structure, and inform the decision to perform condition-based maintenance. The use of piezoelectric elements as actuators in SHM [1], combined with the development of electromechanical impedance measurement for structure characterization [2, 3], has led to the development of high-frequency interrogation for the detection of small, local defects [4].

Impedance-based NDE constitutes a generalization of the SHM process described above through introduction of inter-part comparisons. Instead of comparing a structure to itself over time, potentially-damaged structures are compared to known-healthy reference structures [5]. Here, the quantity being compared is the electrical impedance of a piezoelectric element bonded to the structure. Due to electromechanical coupling, the electrical impedance of

the element is affected by the dynamic vibrational response of the structure. Impedance-based NDE assumes that two structures with the same measured state are equivalent, so that if one is undamaged, so must the other be undamaged.

Impedance-based NDE is of particular interest for structures with complex internal geometry, such as those achievable through additive manufacturing (AM). In previous studies by the authors, bonded piezoelectric elements have been used to detect voids in polymer-based AM specimens [6] [7] and conduct in-situ monitoring of polymer specimens during fabrication [8]. Additionally, previous efforts have shown that the piezoelectric element need not necessarily be directly bonded to the specimen, but instead the element can be bonded to a clamp which is then mechanically attached to a specimen [9].

In this work, impedance-based NDE performed using an instrumented clamp is studied in greater detail. In particular, the effect of clamping force on the effectiveness of damage detection through an instrumented clamp is investigated. In order to isolate the effect of clamping force from fabrication-related uncertainty, machined steel blocks are used as test specimens. This improves consistency between samples compared to additively manufactured specimens, and allows a wide range of clamping forces to be investigated without concern of specimen damage or deformation. Using impedance measurements for damaged and undamaged specimens over a range of clamping forces, a relationship between clamping force and sensitivity to defects is developed using common damage metrics.

## BACKGROUND

Impedance-based NDE examines the dynamic vibrational response of a test object and compares that response to some established baseline. The rationale for this comparison is that changes in mass, stiffness, and damping that result from manufacturing defects will manifest as changes in the object's dynamic response, affecting the frequency and magnitude of the object's resonances.

To make clear how the electrical impedance of the piezoelectric is related to the mechanical properties of the part under test, we will consider the case of a monolithic piezoelectric wafer excited in the 31 mode: electrical stimulus is applied across the thickness (3-direction), and strain is developed along the length (1-direction). For other configurations, a similar result can be derived. The basic concept relies only on the developed strain in the piezoelectric element sufficiently exciting the part under test.

First, the constitutive equations for linear piezoelectricity that capture the 31 mode are shown in Equation 1 [10]

$$\begin{aligned} \varepsilon_{11} &= s_{11}^{E}\sigma_{11} + d_{13}E_3 \\ D_3 &= (d^T)_{31}\sigma_{11} + \epsilon_{33}^{\sigma}E_3 \end{aligned} \tag{1}$$

where $\varepsilon_{11}$ is the normal strain in the 1-direction, $s_{11}^{E}$ is the complex elastic compliance constant measured at constant electric field, $\sigma_{11}$ is the normal stress in the 1-direction, $d_{13}$ and $(d^T)_{31}$ are piezoelectric constants, $E_3$ is the electric field strength in the 3-direction, $D_3$ is the charge displacement in the 3-direction, and $\epsilon_{33}^{\sigma}$ is the complex permittivity in the 3-direction measured at constant stress.

For a test object, the dynamic response to excitation at any particular frequency can be approximated by a single degree of freedom system as shown in Figure 1. The parameters of the system can be written as $m_r$, $k_r$, and $\zeta_r$, denoting mass, stiffness, and damping, respectively.

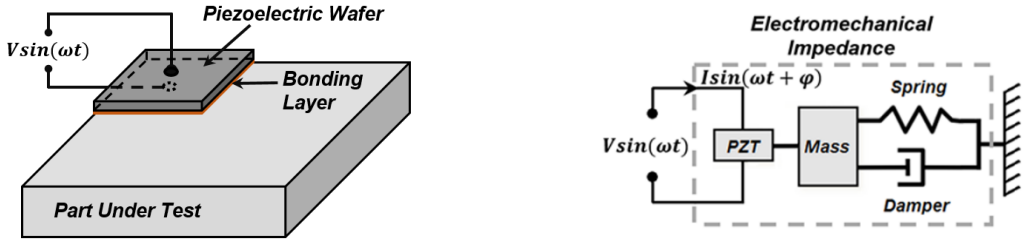


(a) (b)

Figure 1: (a) a piezoelectric transducer bonded to a test object, (b) an abstract system diagram for the arrangement in (a) when excited at a particular frequency [7]

Then, assuming the piezoelectric transducer is perfectly bonded to the test object, Equation 2 shows the electrical impedance of the transducer written in terms of the properties of the piezoelectric and of the test object [2] [11].

$$Z(\omega) = \left[ i\omega \frac{bl}{h} \left( \frac{d_{11}^2}{s_{11}^E} \left( \frac{\tan(kl)}{kl} \left( \frac{Z_{pzt}}{Z_{pzt} + Z_{st}} \right) - 1 \right) + \epsilon_{33}^{\sigma} \right) \right]^{-1} \tag{2}$$

where $Z_{pzt} = -i(bh/l)(s_{11}^E \omega \tan(kl)/kl)^{-1}$ is the piezoelectric transducer impedance under short-circuit conditions, $Z_{st} = 2\zeta_r(k_r m_r)^{1/2} + i(m_r\omega^2 - k_r)/\omega$ is the mechanical impedance of the test object, $k = \omega(\rho s_{11}^E)^{1/2}$ is the wavenumber, $\rho, b, h,$ and $2l$ are the piezoelectric density, width, thickness, and length, respectively.

In order to quantitatively compare impedance signatures, Root-Mean-Square Deviation (RMSD) and a correlation metric ($r$) will be used as damage metrics. Increase in either damage metric value corresponds to divergence between the two signatures being compared, and this divergence will be interpreted as damage. This procedure has been carried out in many other studies, including the ones conducted by the authors of this paper [6], [7], [9]. These metrics can be calculated using Equations 3 and 4.

$$RMSD = \frac{1}{n} \sqrt{\sum \frac{(Z_D - Z_{BL})^2}{Z_{BL}^2}} \tag{3}$$

$$r = 1 - \left| \frac{n\sum Z_D Z_{BL} - \sum Z_D \sum Z_{BL}}{\sqrt{[n\sum Z_D^2 - (\sum Z_D)^2][n\sum Z_{BL}^2 - (\sum Z_{BL})^2]}} \right| \tag{4}$$

where $Z_D$ is the impedance signature of the part being tested, $Z_{BL}$ is the baseline impedance signature, and $n$ is the number of data points in each impedance signature. As defined above, these metrics converge to zero when two signatures are identical, and increase as the signatures become less similar.

## TEST SPECIMEN DESIGN AND INSTRUMENTATION

The test specimens considered in this study, shown in Figure 2, are rectangular steel blocks 4 × 2 × 1 inches in size (101.6 × 50.8 × 25.4 mm). The control specimens weigh 2.28 lb (1.03 kg). Some of the specimens have had damage introduced in the form of a slot milled along one side. In all cases the slot length and width are identical, 4 and 0.5 inches (101.6 and 12.7 mm), while the slot depth is varied to represent various levels of damage severity. The slot depths are 0.1, 0.2, and 0.3 inches (2.5, 5, and 7.5 mm), which produce a mass reduction of 2.5, 5, and 7.5%, respectively, compared to the control specimens.

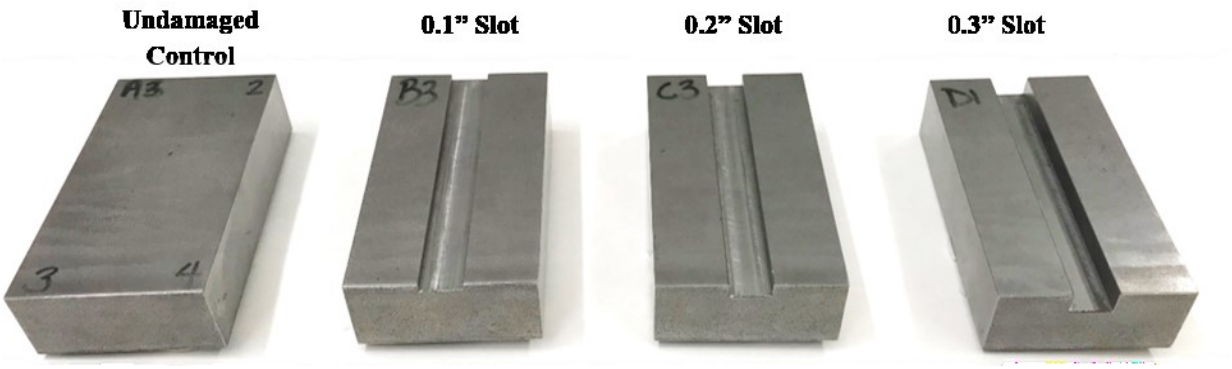


Figure 2: Overview of specimen types. Control specimens are rectangular blocks, and damage is represented by slots milled along one face at several depths to represent damage severity.

Additionally, each block specimen is instrumented with a circular piezoceramic element nominally 1" (25.4 mm) in diameter and 0.1" (2.5 mm) thick. In all cases, the piezoceramic is bonded to the face reverse of the slot in the lower right corner, labeled "4" on the undamaged control block shown in Figure 2.

The instrumented clamp used here, shown in Figure 3, is a small, metal, c-shaped clamp with a threaded rod that can be advanced to adjust the clamping force. On the bottom face, a macro-fiber composite (MFC) piezoelectric element is bonded to provide actuation/sensing capability. On the back face, a strain gauge is bonded to monitor the clamping force. The clamp fits within a volume of 4.1 × 2.5 × 2.4 inches (105 × 65 × 60 mm) when the threaded rod is retracted to minimize the height of the clamp. When fully extended, the clamp will accept an object with a height of approximately 2.9 inches (73 mm).

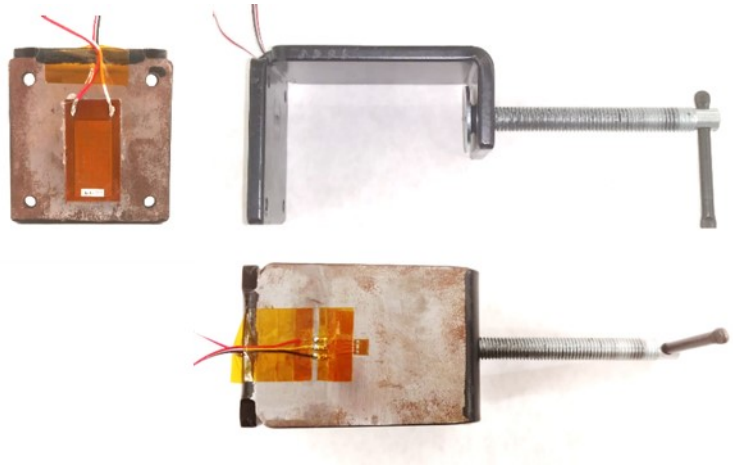

Figure 3: The instrumented clamp. At upper left, the MFC can be seen bonded to the bottom side of the clamp, at lower right, a strain gauge can be seen that is used to monitor clamping force.

For collection of impedance signatures using the instrumented clamp, the block specimens are clamped through their 2 inch dimension with the slot facing inwards, towards the strain gauge. To increase the repeatability of the boundary conditions, a mark was scribed on each block to mark where the threaded rod should contact the block. Additionally, a small ball bearing was placed between the block surface and the end of the threaded rod to simplify

the boundary condition. The bearing both minimizes any torque applied to the specimen as the clamping force is adjusted and allows the contact point to be precisely positioned.

## TEST PROCEDURE

The testing in this paper consists of two main sections: first, a standard impedance-evaluation of specimens using the directly-bonded piezoceramic elements is presented for reference, then an impedance-evaluation of specimens using the MFC patch bonded to the instrumented clamp is conducted at several clamping-force levels: 150, 300, and 600 lb (approximately 665, 1330, and 2670 N).

Prior to testing, the output of the strain gauge bonded to the clamp was calibrated using a force transducer gripped in the same manner as the specimens. The strain gauge output was produced by a Vishay 2110 strain gauge conditioner. A sensitivity of 200 lb/V was selected to make good use of the output voltage range of the conditioner.

During all tests, the impedance signature was collected using a Keysight E4490A impedance analyzer: a device built to precisely produce and measure sinusoidal voltage and current signals. A typical setup for impedance signature measurement is shown in Figure 4. Evaluations of the impedance of the specimens were made over the range of 10-100 kHz at 20 Hz intervals. This resolution was chosen to minimize measurement time of the full spectrum while providing about 5-6 samples over the width of a typical resonant peak. Additionally, during all testing, the specimens were placed on a foam pad to reduce any effect of the surface during measurement.

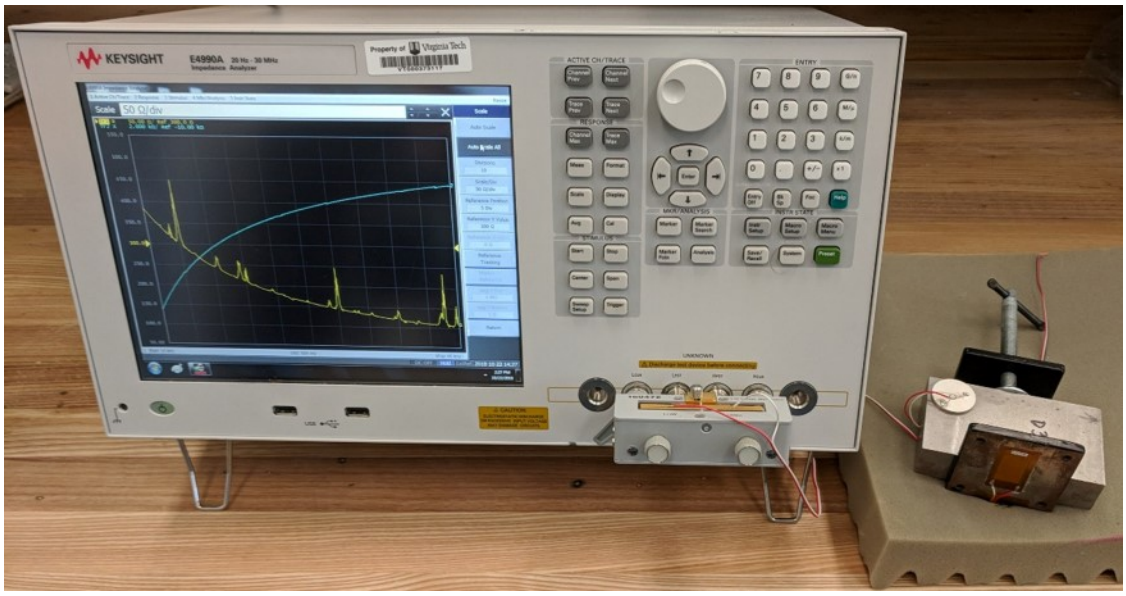


Figure 4: Typical setup for impedance signature measurement. An impedance analyzer gathers data from the MFC patch bonded to the instrumented clamp while attached to a block specimen.

## ASSESSMENT OF SPECIMEN UNIFORMITY

In this section, we will examine the impedance signatures of the blocks on their own, without the clamp attached, as measured by the piezoceramic elements bonded to each specimen. This is the typical procedure for impedance-based NDE, and will provide a basis for comparison when we examine the impedance signatures obtained from the clamped specimens in the following section.

In Figure 5, the impedance signatures of five specimens are shown: two undamaged control specimens and three damaged specimens at three levels of severity. From the control specimen signatures, a baseline signature is

calculated by taking their arithmetic mean. This baseline signature is intended to represent a typical signature for an undamaged specimen. The signature is limited to 40 kHz on the high end because the control signatures showed less agreement above that frequency, and 10 kHz on the low end because there were no resonant peaks observed below that value in initial testing.

It is evident from inspection of the impedance signatures that the control specimens are fairly consistent with one another, while the damaged specimens yield impedance signatures that are both different from the controls and from each other. The peaks around 18 kHz, indicated by the gray regions in Figure 5, appear to be particularly sensitive to the depth of the slot.

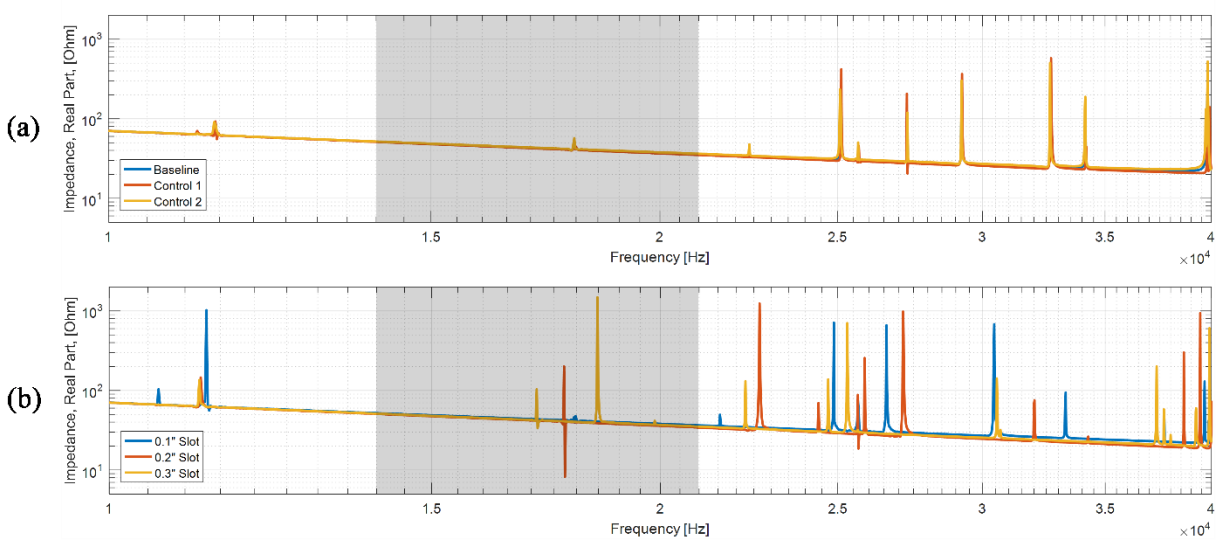


Figure 5: Two signatures from undamaged control specimens are shown in (a), along with a calculated baseline: the arithmetic mean of the control specimen signatures. In (b), a signature from each of the three block specimens with varying levels of damage. The gray areas from 14 – 21 kHz will be examined in more detail below.

To quantify the damage severity, damage metric values are presented in Figure 6. The damage metrics, evaluated over the 10 – 40 kHz interval, show significantly better agreement between the controls and the baseline than between the damaged specimens and the baseline. However, the severity of damage is not apparent from metrics calculated over this wide range. Isolating a region where one resonant peak appears to shift in response to increasing damage severity, Figure 6b, the damage metrics indicate a trend. In the following section, we will examine the same 14 – 21 kHz interval for the clamped measurement.

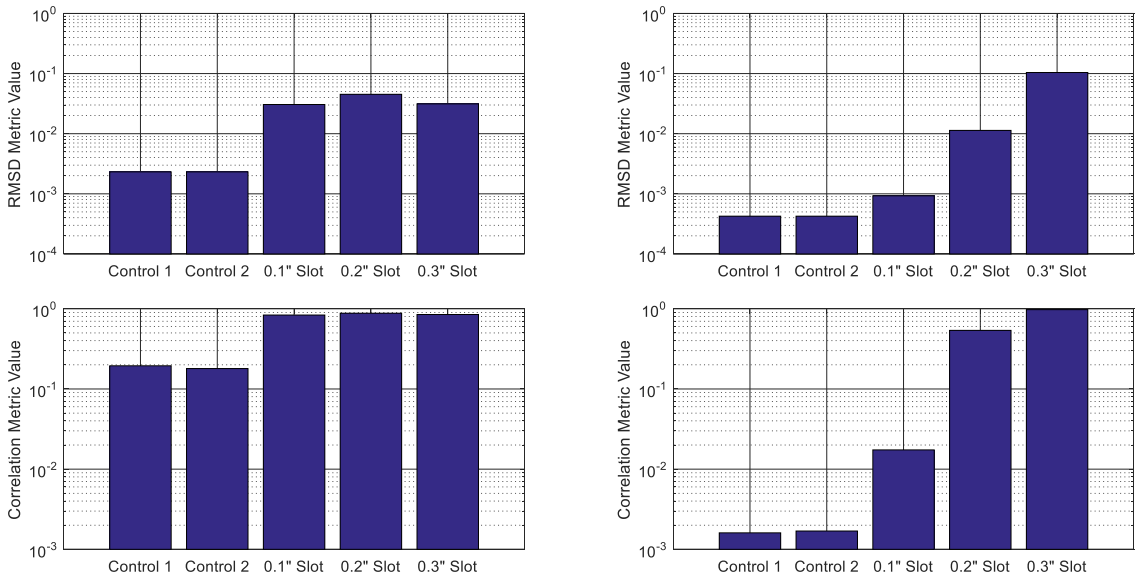


(a) 10 – 40 kHz (b) 14 - 21 kHz

Figure 6: Damage metrics calculated between each block signature and the control group baseline over the intervals (a) 10 – 40 kHz and (b) 14 – 21 kHz. As expected, the damage metrics are small when the control specimens are compared to the baseline, and high when the damaged specimens are compared to the baseline.

## ASSESSMENT OF THE INFLUENCE OF CLAMPING FORCE

In this section, the impedance evaluation will be conducted using the MFC bonded to the instrumented clamp at several levels of clamping force and for all levels of damage severity. The impedance signatures will be presented first, followed by the calculated damage metrics.

Before assessing the changes in the impedance signature due to damage severity, it should be noted that the changes in clamping force will also be expected to change the signature. In Figure 7, the response of the undamaged control specimen is presented as measured by the instrumented clamp for the three clamping force levels.

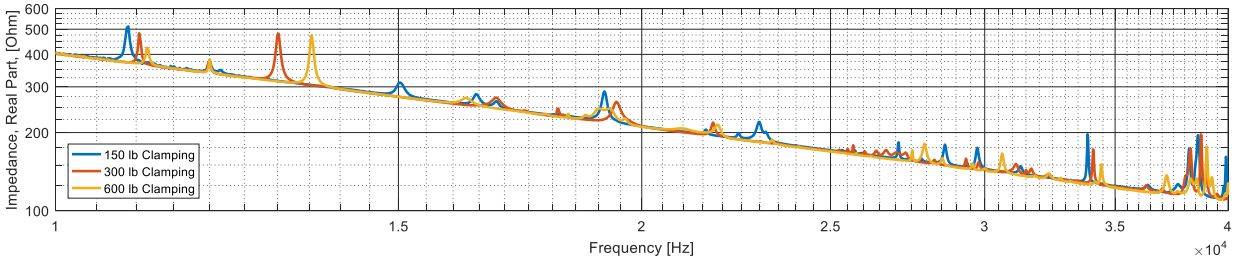


Figure 7: Impedance signature for the undamaged control specimen measured by the clamp MFC over the interval 10 kHz – 40 kHz as clamping force is varied. Peaks at 11 kHz and 34 kHz show a clear increase with clamping force.

At certain frequency ranges in the signature, such as 11 and 34 kHz, a clear trend of increasing peak frequency with clamping force is observed. For other resonant peaks, a clear relationship between clamping force and frequency shifts has not been observed.

Now, we will examine the change in impedance signature with damage severity at each tested clamping force level, shown in Figure 8. In the clamped configuration, the impedance signature is less sensitive to damage severity as compared to measurements from a directly bonded element. Essentially, this is because the measurement is less direct: the damage in the test specimen is being inferred by its effect on the dynamics of the instrumented clamp.

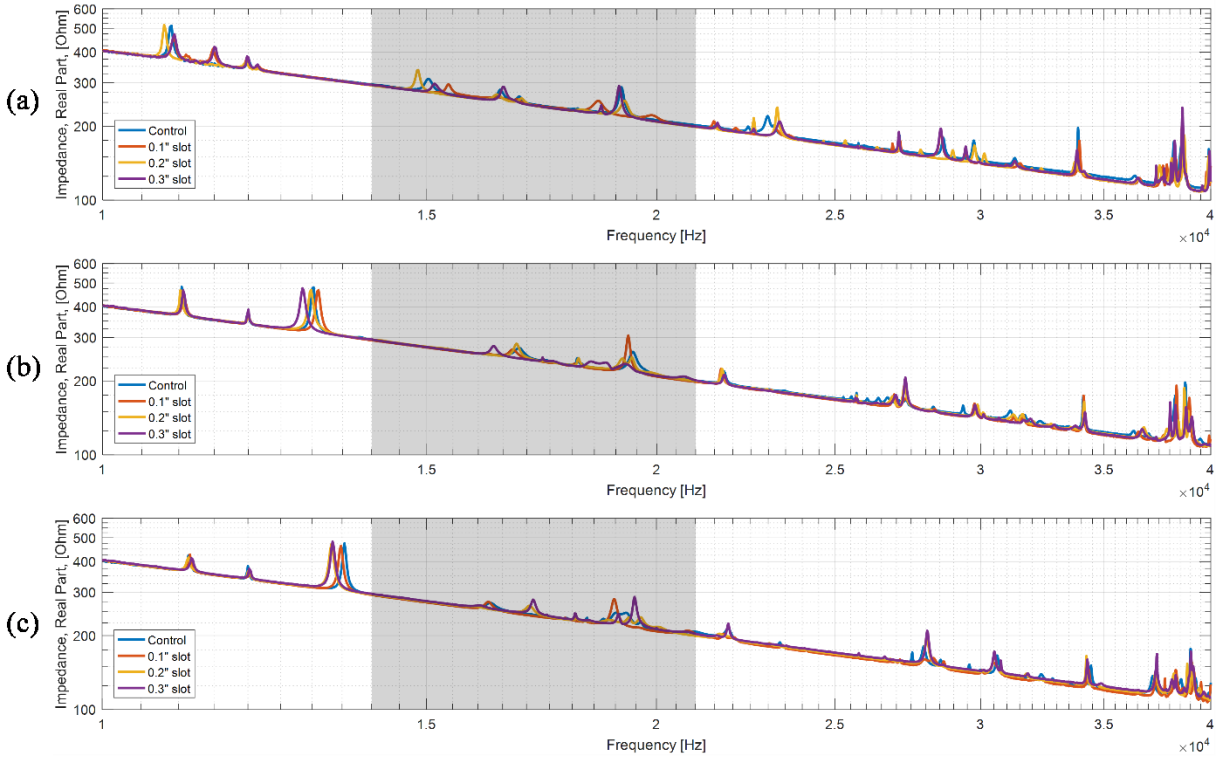


Figure 8: Impedance signatures for each specimen as measured by the instrumented clamp over the interval 10 – 40 kHz for several clamping force levels: (a) 150 lb, (b) 300 lb, and (c) 600 lb. The regions in gray, 14 – 21 kHz, are the same frequency interval indicated in Figure 5.

As done in the previous section, we can evaluate damage metrics first over the entire interval then over a smaller interval where a limited number of peaks reside. The 14 – 21 kHz interval was chosen for comparison because it isolates a group of resonant peaks for both the directly-bonded impedance signatures in the previous section, and the impedance signatures measured by the instrumented clamp here.

In this configuration, the metric values are not as clearly influenced by the level of damage severity as they were in the directly bonded case. In fact, only in the 600 lb case is there an increase in the damage metric values with increasing damage severity. This would indicate that the sensitivity to damage severity increases with clamping force. This indication is also supported by the consistency of the trend in both frequency ranges. The 600 lb case shows an increasing trend with damage severity over both frequency ranges considered, while the 300 lb case shows a somewhat consistent trend, and the 150 lb case shows different trends.

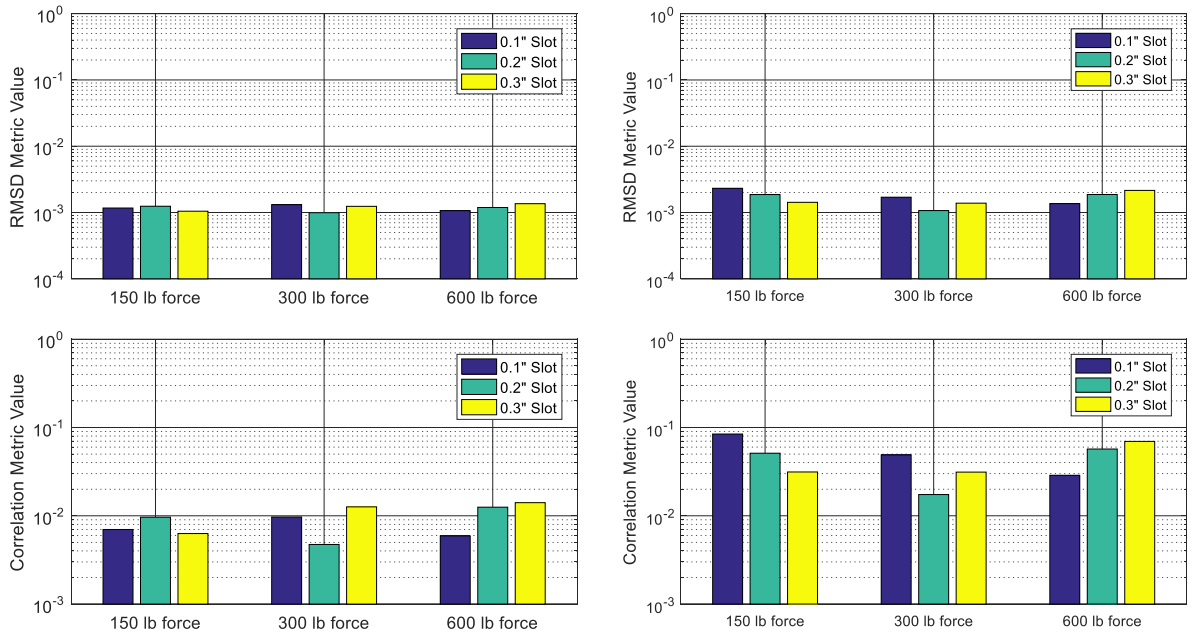


(a) 10 – 40 kHz (b) 14 - 21 kHz

Figure 9: Damage metrics calculated between the damaged specimens and the undamaged control specimen over the intervals (a) 10 – 40 kHz and (b) 14 – 21 kHz. At 150 and 300 lb, the severity of the damage is not apparent from the damage metrics. At 600 lb, the damage metrics increase with the level of damage in both cases.

## CONCLUSIONS

In this work, the effect of clamping force on the sensitivity of a mechanically-attached transducer for impedance-based NDE was investigated. The sensitivity was evaluated by first collecting the impedance signature for the test specimens over a wide range, selecting a smaller range where control specimens showed good agreement, selecting a region that isolated a group of resonant peaks for all damage severities, and finally calculating the values of common damage metrics over that range.

To provide reference values for the damage metrics, the test specimens were initially evaluated with directly-bonded piezoceramic elements. Then, the specimens were re-evaluated using an instrumented clamp to collect the impedance signature. It was found that the directly bonded piezoceramics showed high sensitivity to the damage in the test specimens, showing order-of-magnitude changes in the damage metric at different severity levels over the 14 – 21 kHz frequency range. For the data collected from the instrumented clamp, the damage metric showed much smaller changes between damage severity levels in the same interval, on the order of 50-200% changes in value. In the clamped case, only the highest-force case showed increases in damage metric values with increasing damage severity for the evaluated frequency ranges.

Going forward, further work needs to be done to quantify the uncertainty of the evaluations presented above. By repeating measurements for the same conditions, it would be possible to check whether the observed trends at the 600 lb clamping force are statistically significant. Additionally, considering more force levels and additional specimens would make the results more robust.

**ACKNOWLEDGEMENTS**
The authors would like to thank Mr. T. Komolafe for providing the steel block specimens. Dr. Tarazaga would like to acknowledge the support provided by the John R. Jones III Faculty Fellowship. This material is based upon work supported by the National Science Foundation under Grant Number CMMI-1635356. Any opinions, findings, and conclusions or recommendations expressed in this material are those of the author(s) and do not necessarily reflect the views of the National Science Foundation.

**REFERENCES**

[1] E. F. Crawley and J. De Luis, "Use of piezoelectric actuators as elements of intelligent structures," *AIAA Journal,* vol. 25, no. 10, pp. 1373-1385, 1987.

[2] C. Liang, F. P. Sun and C. A. Rogers, "Coupled Electro-Mechanical Analysis of Adaptive Material Systems-Determination of the Actuator Power Consumption and System Energy Transfer," *Journal of Intelligent Material Systems and Structures,* vol. 8, no. 4, pp. 335-343, 1997.

[3] D. M. Peairs, P. A. Tarazaga and D. J. Inman, "Frequency Range Selection for Impedance-Based Structural Health Monitoring," *Journal of Vibration and Acoustics,* vol. 129, no. 6, pp. 701-709, 2007.

[4] A. S. K. Naidu, S. Bhalla and C. K. Soh, "Incipient damage localization with smart piezoelectric transducers using high-frequency actuation," in *Proceedings of SPIE*, 2002.

[5] K. Worden, C. R. Farrar, G. Manson and G. Park, "The Fundamental Axioms of Structural Health Monitoring," *Proceedings Of The Royal Society A-Mathematical Physical And Engineering Sciences,* vol. 463, no. 2082, pp. 1639-1664, 2007.

[6] M. I. Albakri, L. D. Sturm, C. B. Williams and P. A. Tarazaga, "Impedance-based non-destructive evaluation of additively manufactured parts," *Rapid Prototyping Journal,* vol. 23, no. 3, pp. 589-601, 2017.

[7] C. Tenney, M. I. Albakri, J. Kubalak, L. D. Sturm, C. B. Williams and P. A. Tarazaga, "Internal Porosity Detection In Additively Manufactured Parts Via Electromechanical Impedance Measurements," in *ASME 2017 Conference on Smart Materials, Adaptive Structures and Intelligent Systems*, Snowbird, UT, USA, 2017.

[8] L. Sturm, M. Albakri, C. B. Williams and P. Tarazaga, "In-Situ Detection of Build Defects in Additive Manufacturing via Impedance-Based Monitoring," in *27th Annual International Solid Freeform Fabrication Symposium - An Additive Manufacturing Conference*, 2016.

[9] C. Tenney, M. I. Albakri, C. B. Williams and P. A. Tarazaga, "NDE of Additively Manufactured Parts via Directly Bonded and Mechanically Attached Electromechanical Impedance Sensors," in *International Modal Analysis Conference XXXVI*, Orlando, FL, 2018.

[10] A. H. Meitzler, H. F. Tiersten and W. A. W., *An American National Standard IEEE Standard on Piezoelectricity,* 1987.

[11] G. Park, H. Sohn, C. R. Farrar and D. J. Inman, "Overview of Piezoelectric Impedance-Based Health Monitoring and Path Forward," *Shock Vib. Dig.,* vol. 35, no. 6, pp. 451-463, 2003.